Mathematical Modeling of Tumor Growth, Drug-Resistance, Toxicity, and Optimal Therapy Design

Marios M. Hadjiandreou* and Georgios D. Mitsis

***Abstract*—The combination of mathematical modeling and optimal control techniques holds great potential for quantitatively describing tumor progression and optimal treatment planning. Hereby, we use a Gompertz-type growth law and a pharmacokinetic-pharmacodynamic approach for modeling the effects of drugs on tumor progression in tumor bearing mice, and we combine these in order to design optimal therapeutic patterns. Specifically, we describe colon cancer progression in both untreated mice as well as mice treated with widely used anticancer agents. We also present a pharmacokinetic model to describe the kinetics of drugs in the body as well as detailed toxicity models to describe the severity of side effects. Finally, we propose a promising methodology by which cancer progression in mice with drug resistance can be controlled. By using optimal control, we demonstrate that the optimal planning of the frequency and magnitude of treatment interruptions is key to the control of cancer progression in subjects with resistance and should be further investigated in an experimental setting, which is currently underway.**

***Index Terms*—Cancer modeling, drug holidays, experimental data, optimal control, pharmacokinetics, toxicity.**

I. Introduction

CANCER is a leading cause of death worldwide. Many management options exist for cancer, including chemotherapy, radiation therapy, immunotherapy, and surgery. Issues faced during therapy include metastasis, drug toxicity, interindividual variability, and drug resistance.

The numerous mathematical models of cancer and healthy tissue growth at different levels, from gene expression to the phenomenological description of macroscopic tumor development, have been formulated [1]–[6]. These models have employed concepts from several fields such as systems theory, signal processing and probability theory, and include spatially structured models, physiologically structured, continuous and agent-based, deterministic and stochastic, phenomenological, and mechanistic. The type of modeling methodology to be employed mostly depends on the particular cancer-related process of interest, the point of view of the modeler, as well as the type of data that may be available to perform model estimation.

Many studies have utilized ordinary differential equations (ODEs), which typically involve cancer dynamics alone. Gompertzian growth has been widely used [1], which, unlike exponential growth, also considers the reduced growth rate of the tumor as its size increases. Other ODE models have also been used (e.g., proliferation quiescence models; [2], [3]).

The models of cancer treatment have also been considered: chemotherapy [2], immunotherapy [4], as well as a combination of the above [5]. In most of this study, the reported findings have been based on models which, to begin with, were not validated with experimental data, thus their ability to provide results which can be of clinical value is yet to be demonstrated. Some models included pharmacokinetics [2]; however, no particular drug was examined through real data of effectiveness/toxicity. One previous study [6] used mice data and toxicity was accounted for based on weight loss. This is an improved approach; nevertheless, the model considered in [6] did not take into account the fact that in colon cancer, which was addressed, weight loss is not only a result of drugs, but also of cancer itself [7].

Furthermore, modeling and optimization work needs to account for drug resistance being one of the most important reasons for treatment failure. Some fraction of the cancer cell population may develop drug-resistance and thus evade eradication. Despite the numerous mechanisms to circumvent this problem (e.g., combination treatment), currently no holistic solution exists [8]. Resistance is unavoidable and may lead to a halt of treatment; hence, the problem is not to eliminate the cancerous tumor, but to prolong the patient's life-expectancy [9]. Both stochastic [9], [10] as well as deterministic models have been developed [11] to describe drug resistance. In [12], tumor size is analyzed as a stochastic process and the probability of having no resistant cells appearing is examined. Two-compartment models distinguishing drug-resistant and drug-sensitive cells were developed. The authors of [13] considered infinitely many levels of partial resistance and the corresponding deterministic models were formulated and analyzed in [14]. Due to their high number of free parameters, these often only allow for a purely theoretical analysis. Others have studied drug resistance in a cell-cycle specific context [10]. Models under evolving drug resistance with several killing agents acting separately have also been considered [9]. Most of the resistance work used no real data for

Manuscript received December 11, 2012; revised July 24, 2013; accepted August 5, 2013. Date of publication September 6, 2013; date of current version January 16, 2014. This work was supported in part by the European Regional Development Fund and in part by the Republic of Cyprus through the Research Promotion Foundation (Project Didaktor/0609/48). *Asterisk indicates corresponding author.*

*M. M. Hadjiandreou is with the Department of Electrical and Computer Engineering, University of Cyprus, Nicosia 1678, Cyprus (e-mail: hadjiandreou.marios@ucy.ac.cy).

G. D. Mitsis is with the Department of Electrical and Computer Engineering, University of Cyprus, Nicosia 1678, Cyprus (e-mail: gmitsis@ucy.ac.cy).

Color versions of one or more of the figures in this paper are available online at http://ieeexplore.ieee.org.

Digital Object Identifier 10.1109/TBME.2013.2280189

model development, which is important if the goal is to promote modeling and optimal control as a therapy planning tool in the clinic.

In this paper, we develop pharmacokinetic–pharmacodynamic models describing tumor growth in mice with colon cancer as well as the pharmacokinetic effect of widely used anticancer agents CPT-11, and 5-FU. A model of drug resistance is also developed to describe the tumor and drug dynamics in mice developing resistance to drug docetaxel. Toxicity models which quantify the side-effects of these drugs are also developed. Optimal therapeutic strategies are then developed using optimal control with very promising results which should be explored further in an experimental setting. Unlike other work, here we have made use of experimental data from mice, including tumor data for both untreated and untreated mice, pharmacokinetic data, as well as data from mice developing drug resistance.

The paper is structured as follows: Section II presents mathematical models for 1) cancer progression in mice subjects with colon cancer; 2) mice developing drug resistance; 3) drug kinetics; and for 4) quantifying toxicity in treated mice. Section III examines optimal treatment schedules subject to reduced tumor size and toxicity throughout treatment. Section IV summarizes our findings and the impact of this study in area of computational oncology.

II. Mathematical Modeling

A. Modeling of Cancer Progression in Mice Subjects

Modeling for cancer systems requires two components. The first is an understanding of the system in the absence of treatment and the second is a description of the effects of treatment. A nominal understanding of how cancer progresses is necessary for model construction. Initially, cancer cells typically proliferate in an exponential fashion. The simplest model, first designed to describe tumor growth, is the exponential model, or linear model, if one refers to the ODE rather than to its solution. Assuming that there is no limitation to growth, each cell dividing at a constant rate λ, i.e., with constant doubling time of the cell population given by the relation $T_d = \ln(2/\lambda)$, the model describing cell population (number), T, evolution with unlimited growth is simply [38]:

$$\frac{\mathrm{d}T(t)}{\mathrm{d}t} = \lambda T(t). \tag{1}$$

The size of the cancerous mass is measured experimentally as a volume, though this mass is often referred to in terms of the number of cells (10^6 cells $\approx$ 1 mm^3) [15]. Naturally such a simple model can only describe the very early stages of tumor growth, when no limitation by nutrient supply or mechanical constraints is present. To take account of these natural limitations, and others, the continuous logistic model was proposed as a first improvement. This model is given in [38]:

$$\frac{\mathrm{d}T}{\mathrm{d}t} = kT\left(1 - \frac{T}{T_\infty}\right), \quad k > 0, \quad 0 < T(0) < T_\infty \tag{2}$$

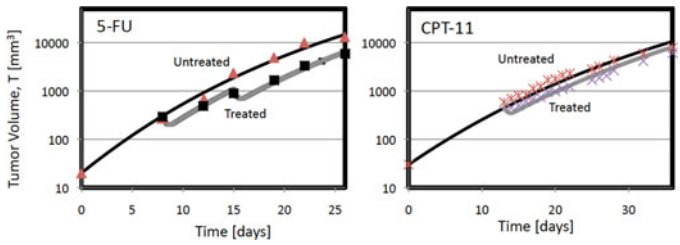

Fig. 1. Tumor growth plotted alongside mice data. Data from untreated mice (∗, ▲) and from mice that received treatment (■, ×) [17].

where k is a rate costant. The model has two equilibrium points: $T = 0$, which is unstable, and $T = T\infty$, which is stable, i.e., the solutions, initially exploding exponentially at a rate k, will eventually converge to the equilibrium value $T = T\infty$.

In this study, we use a Gompertz-type growth equation, which confirms experimental consensus that as the tumor size increases, growth slows as the mass approaches a plateau population [15]. Furthermore, Gompertz-type models are very popular among clinicians dealing with chemotherapy and radiotherapy since these often account for therapy rather than basic tumor growth dynamics. The tumor dynamics in the body as predicted by this type of models is depicted in Fig. 1 with model equations given as

$$\frac{\mathrm{d}T(t)}{\mathrm{dt}} = \frac{1}{\tau_g}\frac{\ln[\theta_g/T_0]}{\ln[\theta_g/2T_0]}T(t)\ln\left[\frac{\theta_x}{T(t)}\right] - L(T(t),C_2(t)) \tag{3}$$

where $T(t)$ is the tumor volume (mm^3) at time t, θ_g is the plateau size (mm^3), τ_g is the tumor doubling time (d), and T_0 is the initial tumor size. The first term represents the increase in cells due to proliferation and L is a function used to describe the decrease in cells due to therapy. When L is 0, then (1) represents the untreated cancer model.

L is linear in T, due to the fact that most drugs have been shown to kill cells by first-order kinetics, i.e., the fraction of tumor cells killed by a drug of fixed concentration is not dependent upon the size of the tumor. The cell-loss term is an affine function of drug concentration at the tumor site $C_2(t)$:

$$L(T(t), C_2(t)) = k_{\mathrm{eff}}(C_2(t) - C_{2\mathrm{thr}})H(C_2(t) - C_{2\mathrm{thr}})T(t) \tag{4}$$

where $C_{2\mathrm{thr}}$ (ng ml^{-1}) is a therapeutic threshold, k_{eff} (d ng ml^{-1}) is the drug kill rate, and H is the Heaviside function: if $C_2(t) - C_{2\mathrm{thr}} < 0$, $H = 0$, if $C_2(t) - C_{2\mathrm{thr}} \geq 0$, $H = 1$. The drug will only be effective if its concentration reaches a threshold. Below this, it has no effect on tumor; however, it still adds to toxicity.

In Fig. 1, our predictions using the system of model (3), (4) are plotted with experimental data from [17]. In [17], both untreated and treated mice with colon cancer were involved. One group of mice received 5-FU with the other receiving CPT-11;, however, each group also involved untreated subjects serving as controls. In order to obtain the subject-specific tumor model for the untreated mice, we formulated and solved (gPROMS ModelBuilder 3.3.1 [39]) a maximum likelihood parameter estimation problem to estimate the doubling time of the tumor during exponential growth, τ_g. The model predictions alongside

TABLE I
PARAMETER VALUES AND STATISTICAL MEASURES FOLLOWING ESTIMATION USING TUMOR [17], [26] AND WEIGHT LOSS DATA [26], WHERE S.D. (STANDARD DEVIATION), CI 95%: 95% CONFIDENCE INTERVAL, AND WR: WEIGHTED RESIDUAL

Parameter	Value	s.d.	CI 95%	WR
***Tumor* ***				
$\tau_{g_{(5FU)}}$	1.88 d	0.045	0.125	6.61
$\tau_{g_{(CPT)}}$	3.00 d	0.253	0.538	0.96
$k_{eff(5FU)}$	$1.20\ 10^{-4}\ \frac{\text{d ng}}{\text{ml}}$	$1.52\ 10^{-5}$	$4.83\ 10^{-5}$	6.58
$k_{eff(CPT)}$	$1.27\ 10^{-3}\ \frac{\text{d ng}}{\text{ml}}$	$1.72\ 10^{-4}$	$3.71\ 10^{-4}$	16.8
Tumor* *				
$\tau_{g_{(CPT)}}$	3.27 d	0.423	0.9301	1.26
$k_{eff(CPT)}$	$3.06\ 10^{-3}\ \frac{\text{d ng}}{\text{ml}}$	0.0001116	0.0002328	22.319
Weight* *				
k_g	0.0163	0.00204	0.00431	21.72
k_{l1}	0.00598	0.000395	0.00083	20.05
k_{l2}	0.000183	$2.65\ 10^{-5}$	$5.59\ 10^{-5}$	21.72

* Using data from [17].
** Using data from [26].

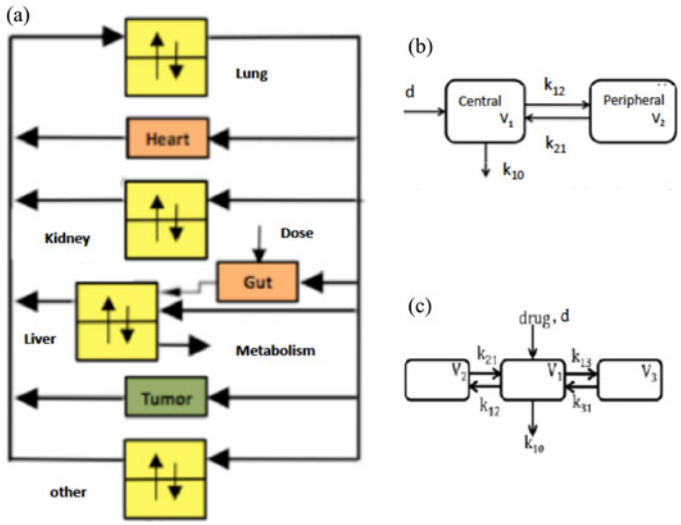

Fig. 2. Panel (a): Physiologically based pharmacokinetic model. Panels (b) and (c): 2- and 3 compartmental models expressing pharmacokinetics in the plasma, tumor, and slowly diffused tissue.

data [17] are depicted in Fig. 1 (untreated), and it can be concluded that the Gompertzian model can provide a good fit to the data of disease progression (see Table I). Standard deviation is one order of magnitude lower than estimated τ_g; thus, there is sufficient accuracy in the estimation. Parameter accuracy was also tested successfully using a t-test in gPROMS.

We have also studied the cancer dynamics with treatment, which we will present next.

B. Pharmacokinetic Modeling

The dynamic effects of drug administration can be described using pharmacokinetic models. Perhaps the most straightforward method for modeling pharmacokinetics is to assume that the body can be approximated as a well-mixed tank. The advantage of this is the small number of parameters that can often be estimated from experimental data. The low-order model is an adequate approximation for compounds with rapid distribution/metabolism characteristics. While this is sufficient for drugs the action of which is based on plasma concentration, or the treatment objective of which is pharmacokinetically driven, a more detailed description of drug distribution is of interest when the site of action or toxicological effect is remote to the plasma. On the other hand, physiologically based (PB) models [18] [see Fig. 2(a)] lie near the other extreme with regards to complexity. According to this approach, differential equations are used to describe concentrations in organs that are assumed well-mixed, and dynamics can be added as needed by subdividing organs into compartments. Mathematically [19]

$$V_{vi}\dot{C}_{vi} = F_i\left(C_c - C_{vi}\right) + \left(k_{tv}C_{ti} - k_{vt}C_{vi}\right) \tag{5}$$

$$V_{ti}\dot{C}_{ti} = -k_{tv}C_{ti} + k_{vt}C_{vi} - r_r \tag{6}$$

where v: vascular and t is interstitial/tissue spaces of tissue i, respectively. The distribution volumes of the drug are given by V_t, C is drug concentration, and F is the blood flow rate. The number of parameters in a PBPK model is significantly higher than a compartmental PK description, and the information necessary to estimate these parameters is typically tissue-specific concentrations of the compound of interest. When available, these data and model structure can provide markedly increased insight into the drug kinetics and any toxicity effects [20], however, due to the detailed information needed these are not commonly used. In between these two extremes lie low-order compartmental models, which we present next. A two-compartmental model describing the kinetic behavior of the drug and its corresponding concentration profile at the cell level is given by [see Fig. 2(b)]

$$\frac{\mathrm{d}C_1(t)}{\mathrm{d}t} = k_{21}C_2(t)\frac{V_2}{V_1} - k_{12}C_1(t) - k_{10}C_1(t) + \frac{\mathrm{d}(t)}{V_1} \tag{7}$$

$$\frac{\mathrm{d}C_2(t)}{\mathrm{d}t} = k_{12}C_1(t)\frac{V_1}{V_2} - k_{21}C_2(t) \tag{8}$$

where $C_1(t)$ and $C_2(t)$ are concentrations in the plasma and tumor site (ng ml^{-1}), respectively; V_1, V_2 are volumes of distribution (ml); d is the dosage (ng d^{-1}); k_{12}, k_{21}, k_{10}: rate constants (d^{-1}).

The two types of therapy were considered [17]: 1) 5-FU was given as an i.v. bolus at a dose level of 50 mg/kg once weekly from Day 8 for 2 weeks and, 2) CPT-11 (i.v. bolus) was given as a single dose at 45 mg/kg on Day 13. The parameters used in the PK model are taken from [17] ($k_{10}^{\mathrm{CPT}} = 13.27$, $k_{10}^{\mathrm{5FU}} = 151.2$, $k_{12}^{\mathrm{CPT}} = 0.276$, $k_{12}^{\mathrm{5FU}} = 5.62$, $k_{21}^{\mathrm{CPT}} = 1.48$, $k_{21}^{\mathrm{5FU}} = 2.31\ \mathrm{d}^{-1}$, $V_1^{\mathrm{CPT}} = 4.85 \times 10^3$, $V_1^{\mathrm{5FU}} = 0.71 \times 10^3$, $V_2^{\mathrm{CPT}} = 8 \times 10^3$, $V_2^{\mathrm{5FU}} = 0.1 \times 10^3$ ml) and the model results show very good agreement with the data for both drugs in terms of drug kinetics (see Fig. 3) as well as in terms of tumor killing rate (see Fig. 1-Treated). The drug-killing parameters were estimated using the maximum likelihood estimation algorithm in gPROMS and the results are shown in Table I.

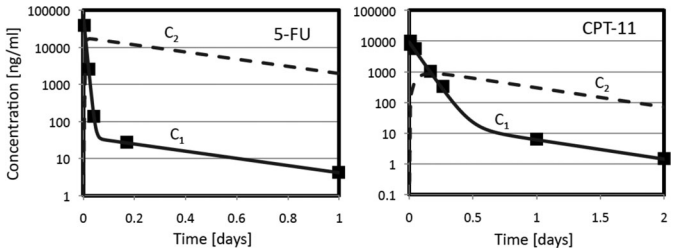

Fig. 3. Plasma concentrations of 5-FU and CPT-11 with mice data (■) following a single dose of 50 mg/kg and 45 mg/kg, respectively (iv. bolus).

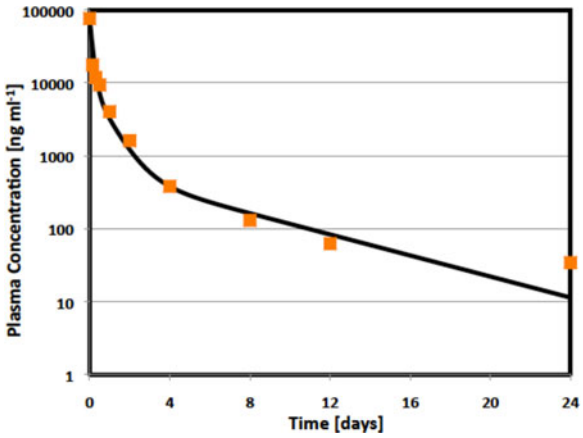

Fig. 4. Model predictions for plasma concentration with experimental data (■) following i.v. bolus administration of docetaxel [20 mg kg-1].

Two-compartmental models present a good approximation of the kinetics of many drugs; however, they are not applicable to some drugs. The pharmacokinetic behavior of docetaxel, for example, is best approximated using a three-compartmental model, which is given by [see Fig. 2(c)]

$$\frac{\mathrm{d}C_1(t)}{\mathrm{d}t} = k_{21}C_2(t)\frac{V_2}{V_1} + k_{31}C_3(t)\frac{V_3}{V_1} - (k_{12}+k_{13})C_1(t) - k_{10}C_1(t) + \frac{\mathrm{d}(t)}{V_1} \quad (9)$$

$$\frac{\mathrm{d}C_2(t)}{\mathrm{d}t} = k_{12}C_1(t)\frac{V_1}{V_2} - k_{21}C_2(t) \quad (10)$$

$$\frac{\mathrm{d}C_3(t)}{\mathrm{d}t} = k_{13}C_1(t)\frac{V_1}{V_3} - k_{31}C_3(t) \quad (11)$$

where $C_1(t)$, $C_2(t)$, and $C_3(t)$ denote drug concentrations in the plasma, tumor site, and other slowly diffused tissues, respectively, V_i denote volumes of distribution, and d is drug dosage. The rate constants $k_{12}, k_{21}, k_{13}, k_{31}$ express the link process between the central and the other compartments and k_{10} denotes other elimination processes.

Fig. 4 depicts the concentration profile of anticancer agent docetaxel along with experimental data [22] in tumor-bearing mice receiving a single dose of a 20 mg kg^{-1} i.v. bolus. This drug has been shown experimentally to exhibit the aforementioned three-compartmental type of kinetics [23] as opposed to other drugs (5-FU, CPT-11), which have been shown to exhibit kinetics best described using two-compartment models. The model

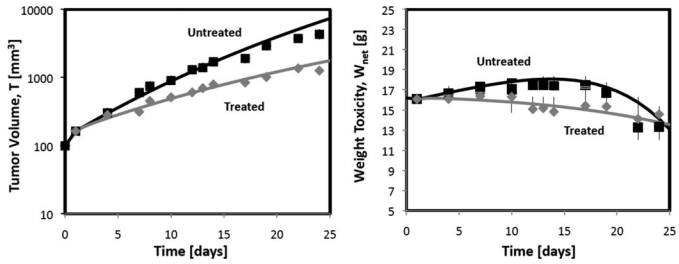

Fig. 5. Left: Tumor growth with data [26] – untreated mice (■) and mice with receiving CPT-11 (♦). Right: Net body weight with data from the same study.

parameters used are from [24] and represent the kinetics as estimated in an experiment involving tumor bearing mice treated with docetaxel. These mice developed resistance to docetaxel; we consider drug-resistance dynamics below (see Section II: drug resistance).

C. Toxicity Modeling

1) Weight Loss Model: The main objective of optimal therapy planning is successful disease control. However, neglecting drug-related toxicity is extremely important as it might prove dangerous or even fatal to the patient.

Some previous studies have considered toxicity [2], [3] but based this on the magnitude of drug concentration only. Because of interpatient and drug variability, large variations can occur across a population, and consequently average exposure (of a generic or even specific drug) as a metric for approximating toxicity may provide little utility. As a more quantitative and experimentally accessible metric, reductions in body weight are often considered in an experimental setting. By modeling reduction this, a constraint on the maximum allowable weight loss can be included in the treatment design algorithm.

A weight loss model may include terms related to loss due to toxicity but also due to cancer itself. The latter has only been accounted for in [16] and it yields a more realistic model that may lead to improved results:

$$\frac{\mathrm{d}W_{\mathrm{net}}(t)}{\mathrm{d}t} = k_g W_{\mathrm{net}}(t) - k_{l1}C_2(t) - k_{l2}T(t). \quad (12)$$

The body weight $W(t)$ is the total mass of the animal which includes the mass of the tumor. The body weight for toxicity purposes, W_{net}, is calculated as $W_{\mathrm{net}} = W(t) - \rho T(t)$, where ρ is tumor density and it approximated as being equal to that of water [25]. This corrects body weight as the tumor burden changes by removing its mass from that of the animal. Body mass grows at a rate k_g and decreases with the drug at a rate constant k_{l1}. The effect of colon cancer on weight is accounted for by $k_{l2}T(t)$.

Fig. 5 depicts body weight dynamics using the model above for both untreated and treated mice with colon cancer (data from [26]). The tumor dynamics for the same mice are also presented. Model parameters were estimated from the data using the maximum likelihood algorithm in gPROMS and are depicted in Table I. Note the effect of the tumor on the weight of untreated mice. These experience a reduction in weight as the tumor grows, even though treatment has not been administered.

TABLE II
FREQUENCIES AND RELATIVE MAGNITUDE OF SELECTED CPT-11 AND 5-FU SIDE EFFECTS [40], [41]

SIDE EFFECT	CPT-11	5-FU
**Diarrhea (1/2)	×	×
**Nausea (1/2)	×	×
***Leukopenia (3/4)	×	□
*Cutaneous (1/2)	□	□
**Vasodilation (flushing)	□	-

Reported in >15% of patients (x), 5–15% (□), <5% (+), 0% and is strongly (***), moderately (**) or weakly (*) undesirable.

The certain types of cancer, including colon cancer may cause a reduction in body weight, and the model captures this important phenomenon.

2) Side-Effect Index: Here, we introduce a methodology for further quantifying drug toxicity in a more rigorous manner. It is based on the severity and frequency of appearance of the individual side effects of each drug within a population, as found by clinical studies. This methodology has been previously proposed [28], [29] for HIV and here it is applied for the first time in the context of cancer modeling. Table II presents the observed side effects at standard dosage for CPT-11 and 5-FU [40], [41]. Note that the actual algorithm that we have implemented uses a total of 57 side-effects; due to space constraints only a selection is presented here. Severity is clearly subjective, e.g., "chills" should be less undesirable than "heart disease." The total side effect of a drug regime at a given time is given as a function of concentrations, the relative magnitude of a side effect, and its observed frequency within a population [42]

$$S_e(t) = \sum_{i=1}^{N} \overline{e_i} \frac{C_2^i(t)}{\overline{C_2^i}} \tag{13}$$

$$e_i = \sum_{j \in J_i}^{N} (q_j, h_{i,j}) i \in N \tag{14}$$

$$\overline{e_i} = \frac{e_i}{\max(e_i)} i \in N. \tag{15}$$

In (13)–(15), $S_e(t)$, represents the magnitude of the side effect of a drug regime at time t, i (i = 1, 2, ..., N) denotes drug index, J_i is the set of side effects related to drug $i, C_2^i(t)$ is the concentration of drug i at time t in the peripheral compartment, $\overline{C_i}$ is the mean concentration of drug i at steady-state at standard dosage, e_i $(\overline{e_i})$ is the magnitude (normalized magnitude) of the side effect caused by drug i at standard dosage, $h_{i,j}$ is the frequency of individuals that present side-effect j when subject to drug i at standard regime, and q_j is the relative magnitude of side-effect j, i.e., "undesirability." This model assumes additivity of the observed frequencies and magnitudes of side effects, and considers that the magnitude of the side-effect index is proportional to the amount of drug administered. The observed frequencies of side effects are modeled using their actual values as found in clinical studies (e.g., 29% for ↓Body weight) [40], [41]. Evaluating the above formulation for CPT- 11 and 5-FU at standard dosage, we conclude that CPT-11 is a more toxic drug when compared to 5-FU. As a result, we would expect optimization studies which utilize this information when formulating a combination therapy for 5-FU/CPT-11 to present schedules which administer more 5-FU than CPT-11 throughout treatment duration, given that both drugs exhibit similar anticancer effect. We will examine this point in Section III. The total side-effect index of a drug regime, S_e^T, initiated at time t_0 up until time t_f is given as the integral of the side-effect index during this time interval.

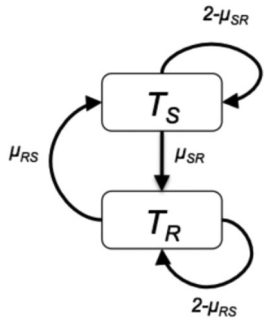

Fig. 6. Mechanism of drug-resistance in the formulated model.

D. Mathematical Model of Drug Resistance

Drug resistance is one of the major drawbacks of chemotherapy. Despite an increasing number of experimental/clinical studies as well as theoretical work on treatment interruptions as a means to fight resistance in HIV [27]–[29] these have not been studied extensively in cancer. In HIV, treatment breaks have been studied to reduce toxicity and facilitate the interplay between the drug-sensitive and drug-resistant HIV strains to control their growth. In cancer, this interplay arises as a result of the reduced fitness of the resistant strain; this has been studied experimentally for the case of drug-resistant cancer cells [30]. Although the two cancer populations are not in direct competition with each other, the battle for nutrients leads to dynamics that are in principle the same as those observed in competition. Next, we present our study on drug resistance and treatment interruptions as a treatment strategy.

Experimental data from drug-resistance tumor studies [31] were used in model development. Specifically, we deal with a mice developing resistance to drug docetaxel. A 3-compartmental pharmacokinetic model for this drug was presented earlier. Two compartments consisting of drug-sensitive and drug-resistant cells were considered with the numbers of cells in the sensitive and resistant compartments denoted by T_S and T_R, respectively. Total cancer load is denoted by T_T $(T_T = T_S + T_R)$. Once a sensitive cell undergoes cell division (see Fig. 6), the mother cell dies and one of the daughters remains sensitive. The other changes into a resistant cell with probability μ_{SR}, where $0 < \mu_{SR} < 1$. Similarly, when a resistant cell undergoes cell division, the mother cell dies, and one of the daughters remains resistant. It has been shown experimentally [32] that a resistant cell may mutate back into a sensitive state with probability μ_{RS}. Denoting the inverses of the transit times of cells through the sensitive and resistant populations by α,

then

$$\frac{\mathrm{d}T_s\,(t)}{\mathrm{d}t} = -aT_s\,(t) + (1-u(t))(2-\mu_{SR})aT_S(t) + \mu_{RS}a\phi T_R(t) - r_1T_ST_R \quad (16)$$

$$\frac{\mathrm{d}T_R\,(t)}{\mathrm{d}t} = -a\phi T_s\,(t) + (2-\mu_{RS})a\phi T_R(t) + (1-u(t))\mu_{SR}aT_S(t) - r_2T_RT_S \quad (17)$$

$$T_T(t) = T_S(t) + T_R(t) \quad (18)$$

where the first terms on the right-hand side represent mother cell death, the second terms describe the return flows into the compartments, the third terms correspond to the cross-over flows between compartments, and φ is a relative fitness factor for the drug-resistant population. The model is based on [9] and an explanation of the mechanisms involved can be found there. However, the aforementioned model includes important improvements to that work. Specifically, it has been shown experimentally [30] that the drug-resistant cancer cells, which have undergone several mutations and developed resistance to drugs, are less "fit" compared to the drug-sensitive strain in terms of their growth rate given ample natural resources (oxygen, glucose, etc) as well as their ability to compete for any natural resources. This phenomenon is well documented in the experimental literature and the drug-resistant tumor population eventually decreases in a drug free medium as the drug-sensitive strain grows. These important considerations are included in the model through the relative fitness (φ) and competition constants (r_1 and r_2, where $r_1 < r_2$).

In the aforementioned model , drug therapy is quantified by $u(t)$, which corresponds to drug efficacy ($\in$ [0, 1], with 0 and 1 indicating no treatment and full treatment, respectively). It is assumed that the drug has no effect on resistant cells. Drug efficacies are often used in mathematical modeling and are a function of the concentration and effectiveness of the drug. The drug efficacy of an anticancer agent is [33]

$$u(t) = \frac{C\,(t)}{C\,(t) + \omega \mathrm{IC}_{50}} \quad (19)$$

where $C(t)$ denotes drug concentration at the tumor site and IC_{50} represents median inhibitory concentration. We assume that IC_{50} as measured by phenotype assays *in vitro* is equivalent to the IC_{50} *in vivo* [34]; hence, $\omega = 1$. IC_{50} for docetaxel (see Fig. 4) was set to 4.12 ng ml^{-1} [35] and the concentration was predicted using the model in (9)–(11).

The results of the aforementioned model are plotted against experimental data for tumor-bearing mice developing resistance to a 25 mg once weekly schedule of docetaxel. Fig. 7 (top) shows the results for the case of mouse T10. Note the response to treatment during the initial stages of therapy; however, it is evident that following the first two doses, drug-resistant tumor emerges and prevails oversensitive tumor resulting in total cancer load rapid growth. Resistance to docetaxel was also verified experimentally in that study. Model results replicate the response to treatment during initial therapy and the emergence of resistance following successive drug dosages. It can be seen that whereas the sensitive strain is controlled by drugs, the resistant one grows uncontrollably hence resulting in fast tumor growth. If this mouse were to continue receiving the same treatment schedule, cancer numbers would reach the maximum allowable size for mice in experiments short after that, hence treatment failure would occur (4000 m^3; [36]). This is depicted in Fig. 7 (bottom).

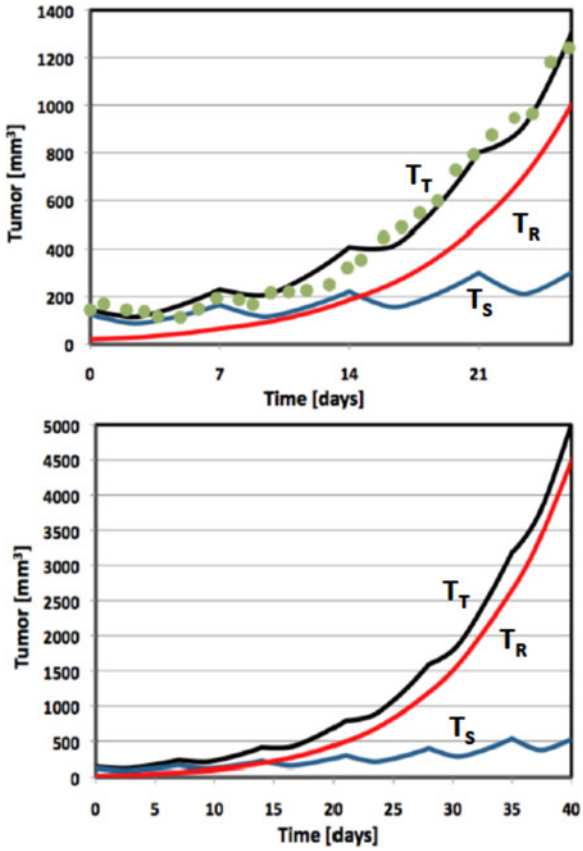

Fig. 7. Top panel: Model predictions for tumor volume with experimental data (•) [31] for mice receiving docetaxel once weekly. Bottom panel: Long-term model predictions for tumor volume according to the schedule in the top panel. Total (black), drug-sensitive (blue), drug-resistant tumor (red).

The proposed model captures a number of important phenomena during resistance emergence and replicates data. One such model could be utilized in the investigation of treatment interruptions through optimal control techniques to highlight avenues of attack against cancer.

III. Optimal Control

Cancer treatment design is a field that could benefit from the contributions of researchers in the field of optimal control. Classical feedback principles in control are not directly applicable to most chemotherapy regimens due to the scheduled nature of therapy and the shortage of available measurements. Therefore, the control problem is generally recast as an optimization problem targeting a desired tumor volume trajectory subject to drug dosing constraints [19].

A number of studies have examined schedules of cancer treatment via optimal control techniques. Various treatment types have been used, including chemotherapy as means to deplete cancer cells [2], immunotherapy as a way to boost the immune system, as well as a combination of the above treatments [5]. Most of these studies designed optimal treatments using models, which were neither developed nor validated with real data. Moreover, they did not include the pharmacokinetic behavior of drugs involved, but instead generic drug efficacy terms were used to represent the percentage effectiveness of the drugs following administration. Some studies did make use of this behavior [2]; however, no particular drug was examined using real data of effectiveness/toxicity. Finally, many studies [3] formulated optimal control problems to obtain a schedule that minimizes the final tumor size, which while an intuitive objective, is not necessarily clinically relevant.

An optimal control algorithm (OCP1) that can be used in treatment design is

$$\begin{aligned} \min J(t_f, \mathbf{d}) &= \int_{t_0}^{t_f} [a_1 T(t) - a_2 W_{\text{net}}(t)] \mathrm{d}t \\ \text{s.t. } \dot{\mathbf{x}} &= f(t,\ \mathbf{x},\ \mathbf{d}) \\ T(t) &\le T_{\max},\ N(t_f) \le N_{\text{target}} \\ W_{\text{net}}(t) &\ge W_{\text{net}}^{\min},\ d_{\min} \le \mathbf{d} \le d_{\max},\ t \in [t_0, t_f] \end{aligned} \quad (20)$$

where $d\mathbf{x}/dt = f(t, \mathbf{x}, d)$ is the model describing tumor dynamics (3), (4), (7), (8), (12), t $\in [t_0, t_f]$ sets the finite horizon of the optimization, $d_{\min} \le d \le d_{\max}$ sets bounds on the maximum tolerated dose (MTD) as found experimentally, and $T(t_f) \le T_{\text{target}}$ sets an end-point constraint for tumor size. A path-constraint in the form of $T(t) \le T_{\max} = 4000$ mm^3 prevents tumor growth in excess of a maximum allowable size before the mice is euthanized [36]. Similarly, $W_{\text{net}}(t) \ge W_{\text{net}}^{\min} = 12.8$ g marks the maximum allowable weight loss as set in experimental protocols [37]. Weighting values a_1 and a_2 penalize extended use of the drug. Unlike other studies solving for minimum tumor burden at a final time only, this algorithm minimizes tumor throughout treatment. Moreover, the path and end-point formulations add further constraints to the tumor and weight trajectories both throughout and at the end of treatment. This considers a more clinically relevant approach for treatment design.

The results for the optimal treatment of the case study presented in Fig. 5 are depicted in Fig. 8 (left panel). It can be seen that the therapy designed using optimal control is successful in maintaining tumor at reduced sizes throughout therapy, driving the final volume to desired levels at the end of treatment. The latter is considerably lower than the size obtained using the treatment in the original study (60 mg kg^{-1}; 1270 mm^3), thus the schedule controls tumor growth within the same horizon more efficiently. In doing this, the dosages administered do not exceed the MTD for drug CPT-11 and the inevitable weight loss is within acceptable limits.

Having investigated the use of the weight loss model in the quest for minimal toxicity, we will now examine the use of the

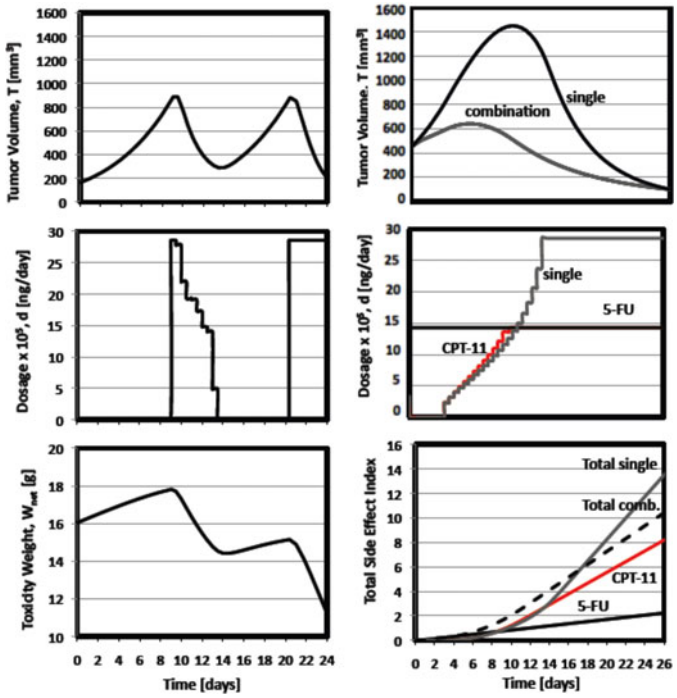

Fig. 8. Left panel: Optimal control using the weight loss model for monotherapy with CPT-11 (left panel). Right panel: Optimal control using the side-effect index for (a) monotherapy with CPT-11 (grey line) and (b) combination therapy with 5-FU (black line) and CPT-11 (red line).

side-effect index formulation. The optimal control problem is formulated for the case study in [17] [see Fig. 1 (right)] and is referred to as OCP2:

$$\begin{aligned} \min J(t_f, \mathbf{d}) &= \int_{t_0}^{t_f} [a_1 T(t) + a_2 S_e(t)] \mathrm{d}t \\ \text{s.t. } \dot{\mathbf{x}} &= f(t, \mathbf{x}, \mathbf{d}) \\ T(t) \le T_{\max}, N(t_f) &\le N_{\text{target}} \\ d_{\min} \le \mathbf{d} \le d_{\max}, t &\in [t_0, t_f] \end{aligned} \quad (21)$$

where $\dot{\mathbf{x}} = f\ (t, \mathbf{x}, \mathbf{d})$ represents (1)–(4) and (6)–(8), $t \in [t_0 = 13, t_f = 39$ days], $d_{\min} = 0 \le d \le d_{\max} = 2.86\ 10^5$ ng g^{-1}, and $T_{\text{target}} = 100$ mm^3. The weighting values a_1 and a_2 were set to 1 and 1×10^7. The optimization results for the treatment of the subjects from [17] are depicted in Fig. 8 (right panel-single). It can be seen that the therapy designed using optimal control is once again successful in maintaining tumor at reduced sizes throughout treatment, driving tumor volume to less than 100 mm^{-3}. This is considerably lower than the original tumor at treatment initiation. In doing this, the drug is only given half way into treatment at dosages which do not exceed the MTD for CPT-11. In fact, the total side effect index achieved was 13.5, as opposed to 22.2 which is the index found when the drug is given at its MTD throughout treatment.

Note that using either toxicity model in the optimization, the result is treatment schedules, which successfully control tumor growth while at the same time keeping toxicity at acceptable levels. In the weight loss model, this is verified by the fact that

the weight loss is within the tolerated limits set by experimental guidelines, whereas in the side- effect index case, the index achieved is considerably less than the one achieved at MTD. Both methods utilize real data and are drug specific, hence present an improved approach to methodologies employed to date. Nevertheless, the index method might be considered more advantageous in that it takes into consideration side effects other than weight loss only; this is usually the case in humans treated for cancer; hence, we consider this to be potentially more useful in a clinical setting.

To examine further the methodology for formulating optimal schedules, which utilize information about the behavior of specific drugs as well as their toxicity, we revisit OCP2 described above; however, this time we consider both 5-FU/CPT-11. Combination therapies are widely used in clinical practice to increase treatment efficacy through synergistic effects, reduce drug-resistance, and other. The combination 5-FU/CPT-11 is common in clinical practice for the case of colon cancer [26]. The formulation is similar to OCP2 with the only difference being the value of $d_{\max} = 1.43 \times 105$ ng d^{-1}. Experimental results [26] suggest that the MTD for drugs in combination differs from the MTD of the drug when administered alone.

The results for the combination treatment are depicted in Fig. 8 (right panel-combination). In a similar manner to monotherapy, tumor growth is inhibited considerably resulting in reduction in its size. In doing this, the optimal schedule administers more 5-FU than CPT-11. This is expected because as found previously, the latter is associated with a higher degree of toxicity at standard dosage and the two drugs exhibit similar anticancer effects as seen by the side-effect index work aforementioned. This result could not have been possible if the drug-specific side effects were not considered (note that 5-FU and CPT-11 also share the same MTD as suggested by experimental studies). This is an important consequence of being able to incorporate drug-specific toxicity model terms in the optimal control problem. In fact, ignoring the toxicity parameter ($\alpha_2 = 0$), yields a treatment which administers both drugs at high dosages. Moreover, the total toxicity for this treatment was 10.4, which is lower than the one achieved at MTD (13.3), but also considerably lower than the CPT-11 monotherapy schedule above (13.5). This is a result of the administration of 5-FU, which is associated with lower toxicity. Finally, as can be seen in Fig. 8 (right panel), combination therapy also appears to be more effective in terms of tumor depletion, inhibiting growth to a greater extent when compared to monotherapy, thus verifying experimental results [26] which support use of combination therapies. We consider these results promising and encouraging for further mathematical modeling and optimization attempts, which utilize experimental and/or clinical information and data in an attempt to obtain clinically relevant results.

A. Drug Resistance: Are Optimized Treatment Breaks the Solution?

In this section, we present results on the treatment of mice exhibiting drug resistance as described earlier (see Fig. 7) using optimal control and investigate whether the optimal management of the frequency and magnitude of treatment breaks can control tumor growth.

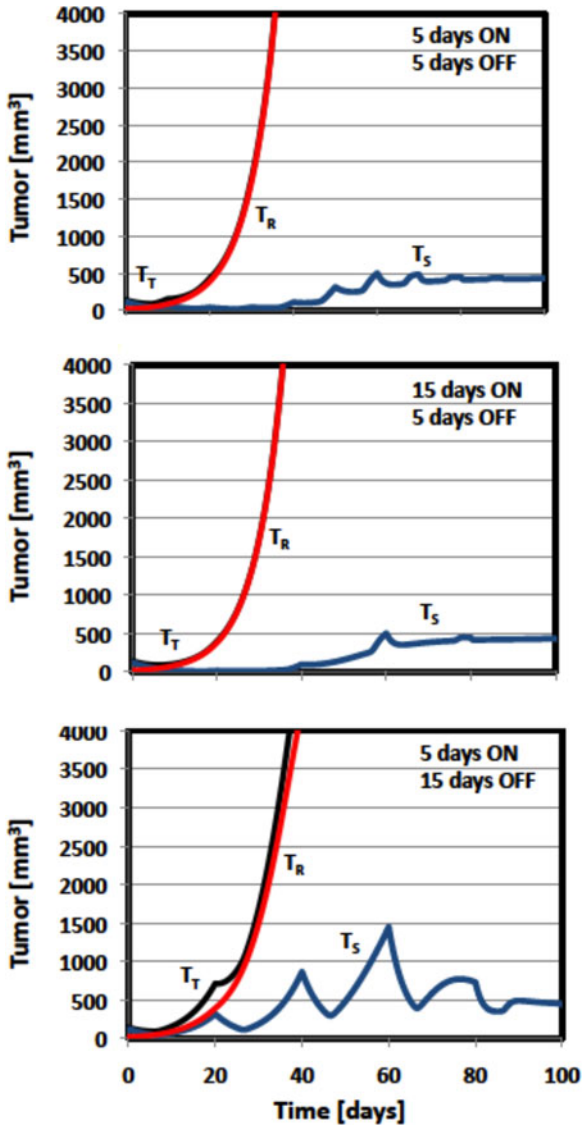

Fig. 9. Chemotherapy with treatment interruptions (not Optimized). Drug-dosage is fixed at the maximum tolerated dosage of docetaxel. Tumor reaches maximum allowable tumor size in animals (4 000 mm^3) very quickly and is not controlled. Total (black), drug-sensitive (blue), drug-resistant tumor (red).

First, we present model simulation results with different combinations of ON and OFF treatment at the maximum tolerated dosage of the drug as found experimentally [31]. We used: 1) 5 days ON, 5 days OFF; 2) 15 days ON, 5 days OFF; and 3) 5 days ON, 15 days OFF and the results are depicted in Fig. 9. In all cases the drug-resistant cancer population is not controlled, in fact the maximum allowable size of tumor in an experimental setting is reached 40 days after treatment initiation.

Now, we present the results of our optimal control study. Here, we examine an optimal ON/OFF treatment schedule based on the minimization of the total tumor size while penalizing extended use of the drug. The administered dosage was fixed to the maximum tolerated dose of docetaxel and treatment intervals were allowed to vary. The treatment levels were fixed during

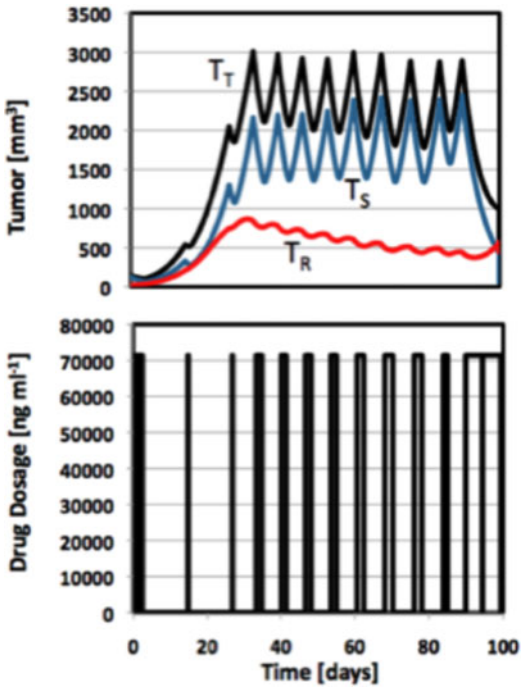

Fig. 10. Top panel: Total (black), drug-sensitive (blue), and drug-resistant (red) tumor trajectories following optimal administration of docetaxel using optimal control. Bottom panel: Optimal administration of docetaxel. Drug dosage is administered at maximum tolerated dose during ON treatment.

the optimization to simplify the optimization problem. On top of this, administration of fixed drug dosages over treatment intervals makes sense as it helps better compliance from patients in a potential administration.

The results of the optimal control-derived therapy are depicted in Fig. 10, where it can be seen that the optimal management of the magnitude and frequency of the treatment breaks during chemotherapy is key for tumor control, hence treatment success. Specifically, optimal management of drug holidays exploits the different characteristics of the drug-sensitive/resistant strains; as a result, neither the sensitive nor the resistant strain grows in an uncontrollable manner and the total cancer load remains at all times below the maximum allowable size. In doing this, the dosages administered do not exceed the maximum tolerated doses for docetaxel administration in mice. This result may be explained as follows: when therapy is administered, it is clear that the resistant strain has an advantage over the sensitive one and will grow faster. The opposite is true in the absence of therapy due to the reduced fitness of the former in terms of its ability to compete for nutrients and grow; hence, the sensitive strain will prevail in this case. Taking advantage of the competitive nature of the two strains so as to prevent their uncontrolled growth using optimized treatment interruption schedules has, in our opinion, great potential and should be explored further.

IV. Discussion and Conclusion

Despite a long history of theoretical work in modeling cancer and optimizing therapy, its practical application has been arguably rather negligible. This stems to a great extent from the lack of collaboration of modelers with clinicians. Most studies to date have based their findings on models which were never developed alongside data or validated and, hence, are often paid little attention by clinicians.

As a result, the primary aim of our study is to utilize, to the extent possible, all information and data available from clinical practice and experiments in order to construct models which represent reality more closely and which may be used in optimal treatment design. Specifically, herein we presented models and control algorithms alongside experimental data from mice. Each of these models is very important in an optimal design framework. Specifically, we presented models for:

1) Mice not receiving any therapy in order to model the untreated cancer dynamics. The exponential growth of cancer cells during the first stages of the disease when nutrients are available, as well as the slowing down of growth as the tumor size increases is shown in the model results.
2) Mice receiving therapy with CPT-11/5-FU. The killing effect of each drug was explicitly included in the model and its magnitude was estimated from data. In both cases, the results successfully represent cancer dynamics during this period.
3) Mice receiving treatment with docetaxel and developing resistance to this drug. Model results successfully predict drug resistance following repeated cycles of docetaxel treatment. The model for drug resistance also takes into consideration the reduced fitness of the drug-resistant cancer population in terms of its ability to compete for natural nutrients with the "fit" drug-sensitive strain.
4) Drug-specific pharmacokinetics in tumor bearing mice, which has been omitted in most studies to date. We have presented a two-compartmental model to describe the kinetics of 5-FU and CPT-11, as well as a three-compartmental model to describe the drug kinetics of docetaxel. In all three cases, we used drug-specific kinetic data and parameter values were taken from the original experimental studies.
5) Predicting drug-related toxicity. In other formulations to date, toxicity was generally assessed by an inferred or generalized toxicity term, handled by constraining input magnitude or rate rather than the measurable and specific toxic effect validated with real data that may be specific to a particular drug-tumor pair. The use of toxicity models based on real data can lead to improved predictions, especially in the case of combination therapy, where one drug may be chosen to be administered at a higher dose (or more frequently) over the other as a result of milder toxicity (e.g., 5-FU in this study). Our approach to model weight loss, which is typically used as a toxicity metric in experiments, not only as a result of toxicity but also as a result of the cancer itself, has been the first attempt to incorporate this important phenomenon.
6) Use in optimal control algorithms with 1) dosage constraints to minimize toxicity; 2) path and end-point tumor constraints to minimize the tumor burden, and 3) weight loss constraints to minimize body weight loss, which is

a result of both toxicity as well as cancer itself. An optimal control case was presented for mice with and without drug resistance. We also showed that combination therapy (CPT-11/5-FU) appears to be more advantageous than monotherapy (CPT-11 only) both in terms of lower toxicity as well as in terms of tumor depletion. This result confirms experimental consensus that favors combination therapy.

Finally, an important result was shown. Drug resistance is one of the most important reasons behind treatment failure, and a solution to this treatment barrier has not yet been demonstrated with certainty. The results show that the key to overcoming resistance and controlling progression is by exploiting the interplay between the drug sensitive and resistant cells through optimized therapy interruptions.

A. Model Selection and Limitations

Over the many years of cancer research, many types of model have been used to represent tumor and healthy cell proliferation. Spatial or not, physiologically structured or not, continuous or agent-based, stochastic or deterministic, phenomenological or mechanistic? These are some important questions which need to be considered in each case. Since cancer is an extremely complex biological phenomenon that occurs in many levels, it is not feasible yet to fully describe all these multilevel processes quantitatively; this is one of the main goals of computational oncology. One of the limiting factors to achieve this long-held goal is often the lack of adequate experimental and/or clinical data obtained from all the aforementioned levels with the required time resolution.

If anything is known of a geometrical structure of the tissue, and if diffusion phenomena (of cells, of locally produced molecules, or of externally delivered drugs) are at stake, then spatially structured models should be used [43]. This is true for models of tumour invasion, in particular gliomas (brain tumours), that are known to evolve with radial diffusion from a localized point in brain, invading the surrounding tissue within the skull. However, often no clear space structure emerges; concentrations of drugs may be taken in first approximation as spatially homogeneous in a given cell compartment; similarly, tumour and healthy cell populations, of different maturation stages, together with vessels, immune cells, possibly acellular necrotic zones, look very mixed up when observed with a microscope, so that space is not always a relevant structure variable for model design in cancer growth. In this case, a nonspatial model should be used.

Therefore, as there is clearly no universal cancer model that could be applied to all cases, we strongly believe that model selection should be based on cancer type, the type of experimental data that may be available and most importantly the main aim of each study.

We are confident that for the purpose of the study to test a promising treatment methodology using animal data (nonhuman and nonmetastatic) and optimal control algorithms, the use of a Gompertz model is well justified, albeit the limitations that may exist. It is a rather different problem to represent, on the one hand tissue growth with the idea to describe all phenomena determining hyperplasia, local, and later remote invasion of a budding tumour, and on the other hand cell population dynamics of the same tumour with control targets, in the perspective of using pharmacological means known to inhibit tumor growth.

Despite their simplicity, Gompertz-type models are very popular because they have been shown to be appropriate for the prediction of the average growth behavior of a tumor in several settings. The fact that they can also be used in optimal control algorithms during treatment optimization work, further justifies their use in our study.

We believe that this study is of great importance and the methodology described herein very promising and worth exploring further in an experimental setting as a first step before clinical testing. We are convinced that this is the main route forward. Mathematical and clinical optimality are not necessarily equivalent and the eventual use of a treatment is in the clinic. Toward this direction we are currently testing the proposed methodology in transgenic mice and we will present the findings in a future study.

References

[1] R. Martin and K. L. Teo, *Optimal Control of Drug Administration in Cancer Chemotherapy*. River Edge, NJ, USA: World Scientific, 1994.

[2] P. Dua, V. Dua, and E. N. Pistikopoulos, "Optimal delivery of chemotherapeutic agents in cancer," *Comput. Chem. Eng.*, vol. 32, pp. 99–107, 2009.

[3] D. Barbolosi and A. Iliadis, "Optimizing drug regimens in cancer chemotherapy: A simulation study using a PK-PD model," *Comput. Biol. Med.*, vol. 31, pp. 157–172, 2001.

[4] L. G. de Pillis and A. E. Radunskaya, "A mathematical tumor model with immune resistance and drug therapy: An optimal control approach," *J. Theor. Med.*, vol. 3, p. 79, 2001.

[5] A. d'Onofrio and A. Gandolfi, "Tumor eradication by antiangiogenic therapy: Analysis and extensions of the model by Hahnfeldt *et al.*," *Math. Biosci.*, vol. 191, pp. 159–184, 2004.

[6] J. M. Harrold and R. S. Parker, "Clinically relevant cancer chemotherapy dose scheduling via mixed-integer optimisation," *Comput. Chem. Eng.*, vol. 4, pp. 2042–2054, 2009.

[7] *Colon Cancer: Signs and Symptoms*, Mayo Clinic, Scottsdale, AZ, USA, 2007.

[8] J. H. Goldie, "Drug resistance in cancer: A perspective," *Cancer Metastasis Rev.*, vol. 20, pp. 63–68, 2001.

[9] U. Ledzewicz and H. Schattler, "Drug resistance in cancer chemotherapy as an optimal control problem," *Discr. Continuous Dynamical Syst.*, vol. 6, pp. 129–150, 2006.

[10] J. J. Westman, B. R. Fabijonas, D. L. Kern *et al.*, "Cancer treatment using multiple chemotherapeutic agents subject to drug resistance," in *Proc. 15th Int. Symp. Mathem. Theory Netw. Syst.*, 2002.

[11] M. I. Costa, J. Boldrini, and R. Bassanezi, "Drug kinetics and drug resistance in optimal chemotherapy," *Math. Biosci.*, vol. 125, pp. 191–209, 1995.

[12] A. J. Coldman and J. H. Goldie, "A model for the resistance of tumor cells to cancer chemotherapeutic agents," *Math. Biosci.*, vol. 65, pp. 291–307, 1983.

[13] J. Smieja and A. Swierniak, "Different models of chemotherapy taking into account drug resistance stemming from gene amplification," *Int. J. Appl. Math. Comput. Sci.*, vol. 13, pp. 297–305, 2003.

[14] A. Swierniak, A. Polanski, M. Kimmel *et al.*, "Qualitative analysis of controlled drug resistance model—Inverse Laplace and semigroup approach," *Control Cybern.*, vol. 28, pp. 61–75, 1999.

[15] L. Norton, "A Gompertzian model of human breast cancer growth," *Cancer Res.*, vol. 48, pp. 7067–7071, 1988.

[16] M. M. Hadjiandreou and G. D. Mitsis, "Towards tumor growth control subject to reduced toxicity," in *Proc 2012 Amer. Control Conf.*, Montreal, Canada, Jun. 27–29, 2012, pp. 5592–5597.

[17] M. Simeoni, P. Magni, C. Cammia *et al.*, "Predictive pharmacokinetic-pharmacodynamic modeling of tumor growth kinetics in xenograft models

after administration of anticancer agents," *Cancer Res*., vol. 64, 2004, pp. 1094–1101.
[18] H. S. Chen and J. F. Gross, "Physiologically based pharmacokinetic models for anticancer drugs," *Cancer Chemother. Pharmacol*., vol. 2, pp. 85–94, 1979.
[19] F. Doyle, L. Jovanovic, D. Seborg *et al*., "A tutorial on biomedical process control," *J. Process. Control*., vol. 17, pp. 571–594, 2007.
[20] K. S. Blesch, R. Gieschke, Y. Tsukamoto *et al*., "Clinical pharmacokinetic/pharmacodynamic and physiologically based pharmacokinetic modeling in new drug development: The capecitabine experience," *Invest. New Drugs*, vol. 21, pp. 195–223, 2003.
[21] M. M. Hadjiandreou and G. D. Mitsis, "Model-based control of cancer progression subject to drug-resistance," in *Proc 2012 IEEE Conf. Decision Control*, to be published.
[22] E. L. Bradshaw-Pierce, S. Eckhardt, and D. L. Gustafson, "A physiologically based pharmacokinetic model of docetaxel disposition: From mouse to man," *Clin. Cancer Res*., vol. 13, pp. 2768–2776, 2007.
[23] S. J. Clarke and L. P. Rivory, "Clinical pharmacokinetics of docetaxel," *Clin Pharmacokinet*., vol. 36, no. 2, pp. 99–114, 1999.
[24] W. Zamboni, S. Strychor, E. Joseph *et al*., "Tumor, tissue, and plasma pharmacokinetic studies and antitumor response studies of docetaxel in combination with 9-NTC in mice bearing SKOV-3 human ovarian xenografts," *Cancer Chemother Pharmacol*, vol. 62, pp. 417–426, 2008.
[25] J. M. Harrold, "Model-based design of cancer chemotherapy treatment schedules," Ph.D. thesis, Univ. Pittsburgh, Pittsburgh, PA, USA, 2005.
[26] Y. Hattori, L. Shi, W. Ding *et al*., "Novel irinotecan-loaded liposome using phytic acid with high therapeutic efficacy for colon tumors," *J. Controlled Release*, vol. 136, pp. 30–37, 2009.
[27] S. G. Deeks and B. Hirschel, "Supervised interruptions of antiretroviral therapy," *AIDS*, vol. 16, no. 4, pp. S157–S169, 2002.
[28] M. M. Hadjiandreou, R. Conejeros, and D. I. Wilson, "Long-term HIV dynamics subject to continuous therapy and structured treatment interruptions," *Chem. Eng. Sci*., vol. 64, pp. 1600–1617, 2009.
[29] M. M. Hadjiandreou, R. Conejeros, and D. I. Wilson, "Controlling AIDS progression in patients with rapid HIV dynamics," in *Proc 2012 Amer. Control Conf*., Montreal, Canada, 2012, pp. 4078–4083.
[30] A. J. Tipping, F. X. Mahon, V. Lagarde *et al*., "Restoration of sensitivity to STI571 in STI571-resistant chronic myeloid leukemia cells," *Blood*, vol. 98, pp. 3864–3867, 2001.
[31] S. Rottenberg, A. O. H. Nygren, M. Pajic *et al*., "Selective induction of chemotherapy resistance of mammary tumors in a conditional mouse model for hereditary breast cancer," in *Proc. Nat. Acad. Sci*., vol. 104, pp. 12117–12122, 2007.
[32] R. T. Schimke, "Gene amplification, drug resistance and cancer," *Cancer Res*., vol. 44, pp. 1735–1742, 1984.
[33] L. M. Wahl and M. A. Nowak, "Adherence and resistance: Predictions for therapy outcome," in *Proc. Roy. Soc. Bio*., vol. 267, p. 835, 2000.
[34] Y. Huang, S. Rosenkranz, and H. Wu, "Modeling HIV dynamics and antiviral response with consideration of time-varying drug, adherence, & phenotypic sensitivity," *Math. Biosci*., vol. 184, pp. 165–186, 2003.
[35] U. Vanhoefer, S. Cao, and A. Harstrick, "Comparative antitumor efficacy of docetaxel and paclitaxel in nude mice bearing human tumor xenografts that overexpress the multidrug resistance protein (MRP)," *Ann. Oncol*., vol. 8, pp. 1221–1228, 1997.
[36] *Guidance Document on the Recognition, Assessment, and Use of Clinical Signs as Humane Endpoints for Experimental Animals Used in Safety Evaluation*, OECD, 2000.
[37] *Animal Experiments in Cancer Research*, Netherlands Inspectorate for Health Protection, Zutphen, The Hague, 1999.
[38] J. Clairambault, "Modeling physiological and pharmacological control on cell proliferation to optimise cancer treatments," *Math. Model. Nat. Phenom*., vol. 4, pp. 12–69, 2009.
[39] *gPROMS*, Process System Enterprise Ltd., London, U.K, 2004.
[40] J. M. Joulia, F. Pinguet, M. Ychou *et al*., "Plasma and salivary pharmacokinetics of 5-FU in patients with metastatic colorectal cancer receiving 5-FU bolus plus continuous infusion with high-dose folinic acid," *EJC*, vol. 35, pp. 296–301, 1999.
[41] (2011). *Irinotecan Side Effects—For the Professional*. [Online]. Available: http//www. Drugs.com
[42] M. Joly and J. M. Pinto, "Role of mathematical modeling on the optimal control of HIV-1 pathogenesis," *AIChE J*., vol. 52, pp. 856–885, 2006.
[43] T. Colin, D. Bresch, E. Grenier, B. Ribba, and O. Saut, "Computational modeling of solid tumor growth: The avascular stage," *SIAM J. Sci. Comput*., vol. 32, no. 4, pp. 2321–2344, 2010.

Authors' photographs and biographies not available at the time of publication.